A New Formulation of Electromagnetic Wave Scattering Using an On-Surface Radiation Boundary Condition Approach

GREGORY A. KRIEGSMANN, ALLEN TAFLOVE, SENIOR MEMBER, IEEE, AND KORADA R. UMASHANKAR, SENIOR MEMBER, IEEE

Abstract—**A new formulation of electromagnetic wave scattering by convex, two-dimensional conducting bodies is reported. This formulation, called the on-surface radiation condition (OSRC) approach, is based upon an expansion of the radiation condition applied directly on the surface of a scatterer. Past approaches involved applying a radiation condition at some distance from the scatterer in order to achieve a nearly reflection-free truncation of a finite-difference time-domain lattice. However, it is now shown that application of a suitable radiation condition directly on the surface of a convex conducting scatterer can lead to substantial simplification of the frequency-domain integral equation for the scattered field, which is reduced to just a line integral. For the transverse magnetic (TM) case, the integrand is known explicitly. For the transverse electric (TE) case, the integrand can be easily constructed by solving an ordinary differential equation around the scatterer surface contour. Examples are provided which show that OSRC yields computed near and far fields which approach the exact results for canonical shapes such as the circular cylinder, square cylinder, and strip. Electrical sizes for the examples are $ka = 5$ and $ka = 10$. The new OSRC formulation of scattering may present a useful alternative to present integral equation and uniform high-frequency approaches for convex cylinders larger than $ka = 1$. Structures with edges or corners can also be analyzed, although more work is needed to incorporate the physics of singular currents at these discontinuities. Convex dielectric structures can also be treated using OSRC. These will be the subject of a forthcoming paper.**

I. Introduction

THE APPROACH PRESENTED here is a high-frequency technique for modeling electromagnetic scattering, radically different from the geometric theory of diffraction (GTD). This new technique, which we call the on-surface radiation condition (OSRC) approach, converts the usual surface integral equation for the scattering problem into either an integration of known quantities or a simple ordinary differential equation for convex two-dimensional targets. It is currently applicable to convex conducting cylinders of arbitrary cross section, yielding codes for both the transverse electric (TE) and transverse magnetic (TM) cases that are suitable for rapid processing by computers in the class of the VAX 11/780. The OSRC approach has been extended to two-dimensional homogeneous dielectric targets, yielding similar analyses. These will be reported in a separate paper [1].

Manuscript received May 31, 1985; revised August 1, 1986. This work was supported in part by NASA Lewis Research Center Grant NAG 3-635 and by National Science Foundation Grant MCS-8300578.

G. A. Kriegsmann is with the Department of Engineering Sciences and Applied Mathematics, Technological Institute, Northwestern University, Evanston, IL 60201.

A. Taflove is with the Department of Electrical Engineering and Computer Science, Technological Institute, Northwestern University, Evanston, IL 60201.

K. R. Umashankar is with the Department of Electrical Engineering and Computer Science, University of Illinois, Chicago, IL 60680.

The OSRC approach was motivated by numerical experiments conducted over the past twenty years aimed at simulating scalar or vector wave propagation and scattering using a finite-difference time-domain (FD-TD) model of the governing wave equation. This type of simulation results in numerical analogs of the incident and scattered waves propagating within a finite, two- or three-dimensional data space of field components positioned at distinct points in a lattice. To bound the numerical domain, but not disturb the simulation of a scatterer embedded in an infinite space, it has been found necessary to introduce a suitable radiation boundary condition at the outermost lattice planes. This boundary condition should allow outgoing scattered waves to exit the numerical data domain without undergoing nonphysical reflection.

Several early investigators employed the Sommerfeld condition (in the time domain) as a local radiation boundary condition to truncate the numerical domain [2]–[5]. Later workers identified and exploited higher order differential operators for this purpose [6]–[11]. These operators appear to fall into two categories. The first, exemplified by the work of Kriegsmann and Morawetz [8] and Bayliss and Turkel [9], uses the asymptotic behavior of the scattered field in cylindrical or spherical coordinate systems to establish a series B_n of operators that, when applied to the scattered field, annihilate the first n terms of the asymptotic series. Bayliss and Turkel further demonstrated that the series B_n can be conveniently generated using a recursive formula. The second category, exemplified by the work of Trefethen and Halpern [11], derives an approximate one-way wave equation in Cartesian coordinates by factoring the dispersion relation of the full wave equation, and providing a rational polynomial interpolation of the resulting square root at selected wave propagation angles. This results in a reflection-free passage of plane waves propagating at these angles through the lattice truncation plane. The number of reflection-free angles and their values can be selected in a systematic manner.

A recent series of numerical experiments involving FD-TD modeling of Maxwell's equations in Cartesian coordinates and two and three space dimensions has been reported [12]–[14]. These experiments utilized the radiation boundary operator published by Mur [10], which is now known to be a Pade (2, 0) approximant as defined by Trefethen and Halpern [11]. For continuous, sinusoidal excitation, it was observed that, if the Mur condition were applied only eight space cells from the outer surfaces of structures spanning up to 96 cells (with each cell spanning approximately 0.1 wavelength), the radar cross section could be modeled with an accuracy of 1 dB or better over a 40 dB dynamic range [14]. The robustness of the numerical experimental data suggested that it might be possible to apply a suitable radiation condition even closer to a scatterer to further reduce the required FD-TD lattice size.

In preparing for the new series of FD-TD numerical experiments, an analysis revealed unexpectedly that substantial simplification of the overall scattering problem would occur for the important class of convex-shaped, two-dimensional, conducting scatterers if the radiation condition were applied *directly on the surface* of a scatterer in this class. Essentially, the original frequency-domain integral equation for the scattered field would be reduced to just a line integral about the scatterer surface contour, where the integrand is either known explicitly (for the TM case) or can be easily constructed via solution of an ordinary differential equation about the surface contour (for the TE case). The prior application of this concept, which we call the OSRC approach, is not evident in the literature.

Subsequent sections of this paper will develop the OSRC theory for two-dimensional, convex-shaped, conducting scatterers for the TM and TE cases. Radiation boundary conditions published by Kriegsmann and Morawetz [8], similar to B_1 and B_2 published by Bayliss and Turkel [9], will be used in this development. (It should be understood that OSRC theory might be developed for the full range of Cartesian or circular coordinate radiation operators, and that operators other than B_1 and B_2 may present specific advantages.) It will be demonstrated that use of a higher order OSRC can yield computed near and far scattered fields which approach the exact solution for several canonical conducting geometries having electrical sizes $ka = 5$ and $ka = 10$. The results indicate that OSRC may present a useful alternative to present integral equation and uniform high-frequency methods for electrically large convex cylinders of arbitrary cross section shape.

II. Formulation of the OSRC Approach (TM Polarization)

We shall consider a plane electromagnetic wave illuminating a two-dimensional, perfectly conducting, convex-shaped cylinder for the transverse magnetic polarization case. The incident wave, propagating at an angle α with respect to the $-x$ axis, is given by

$$\vec{E}_{\text{inc}} = U_{\text{inc}} e^{-j\omega t}\hat{z}; \quad U_{\text{inc}} = e^{jk(x\cos\alpha - y\sin\alpha)} \tag{1}$$

where the unit vector $\hat{z}$ is parallel to the cylinder axis. The parameter ω is the frequency of the incident wave; $k = \omega a/c$; a is a characteristic dimension of the cylinder's cross section; and c is the speed of light in free space. The variables x and y are the corresponding dimensionless Cartesian coordinates in the plane orthogonal to $\hat{z}$. They are scaled with respect to the length a.

The scattered electric field $\vec{E}_s$ is given by

$$\vec{E}_s = U_s(\bar{x})e^{-j\omega t}\hat{z} \tag{2a}$$

$$U_s(\bar{x}) = \int_C \left[G(\bar{x}|\bar{x}')\frac{\partial U_s(\bar{x}')}{\partial \nu'} - U_s(\bar{x}')\frac{\partial G(\bar{x}|\bar{x}')}{\partial \nu'} \right] ds' \tag{2b}$$

where C represents the boundary of the cylinder's cross section; $\partial/\partial\nu'$ denotes an outward normal derivative on C; and G is the free-space Green's function given by

$$G(\bar{x}|\bar{x}') = \frac{j}{4} H_0^{(1)}(kR) \tag{2c}$$

$$R = |\bar{x} - \bar{x}'| = \sqrt{(x-x')^2 + (y-y')^2}. \tag{2d}$$

The vectors $\bar{x}$ and $\bar{x}'$ appearing above are just normalized (x, y) and (x', y'), respectively. Since the cylinder is perfectly conducting, the function $U_s(\bar{x}')$ can be replaced by $-U_{\text{inc}}(\bar{x}')$ in (2b) to obtain

$$U_s(\bar{x}) = \int_C \left[G(\bar{x}|\bar{x}')\frac{\partial U_s(\bar{x}')}{\partial \nu'} + U_{\text{inc}}(\bar{x}')\frac{\partial G(\bar{x}|\bar{x}')}{\partial \nu'} \right] ds'. \tag{3a}$$

Thus, the scattered field is completely determined when $\partial U_s(\bar{x}')/\partial\nu'$ is found. The z-directed surface electric current J is related to this normal derivative by

$$J = \frac{j}{\eta_0 k}\left(\frac{\partial U_s}{\partial \nu'} + \frac{\partial U_{\text{inc}}}{\partial \nu'}\right) \tag{3b}$$

where $\eta_0 = \sqrt{\mu_0/\epsilon_0}$. An expression for the normal derivative will be derived shortly.

First, the far-field expansion of (3) can be obtained by using the asymptotic expansion of $H_0^{(1)}$ as $r \equiv |\bar{x}| \to \infty$:

$$U_s(\bar{x}) = \left[\sum_0^\infty A_n(\varphi, \alpha, k) r^{-n} \right] \cdot \frac{e^{jkr}}{\sqrt{r}} \tag{4}$$

where r and φ are the cylindrical coordinates of $\bar{x}$. The term A_0 in (4) is given explicitly by

$$A_0(\varphi, \alpha, k) = \frac{e^{j\pi/4}}{\sqrt{8k\pi}} \int_C \left[\frac{\partial U_s}{\partial \nu'} - jk\cos\delta\, U_{\text{inc}} \right] e^{-jk\psi}\, ds' \tag{5a}$$

where $\psi = \bar{x}' \cdot \hat{x}$ and $\cos\delta = \hat{\nu}' \cdot \hat{x}$, for $\hat{x} = (\cos\varphi, \sin\varphi)$ and $\hat{\nu}' =$ unit normal to the curve C at s'. The bistatic radar cross section (RCS) is related to A_0 by the expression:

$$\text{RCS} = 2\pi a |A_0|^2. \tag{5b}$$

Next, a sequence of radiation boundary operators $\{B_n\}$, $n = 1, 2, \cdots$ can be constructed which, for any n, annihilates the first n terms in the asymptotic expansion of (4). This can be considered as a way of matching the solution on the radiation boundary to the first n terms of the expansion of the solution exterior to the boundary. When B_n is applied to U_s at a fixed radius $r = R$, the annihilation relationship can be expressed as

$$B_n U_s = O(R^{-2n-1/2}); \quad n=1, 2, 3, \cdots . \tag{6}$$

In this expression, the symbol $O(R^{-m})$ denotes a quantity which decays like R^{-m} as $R \to \infty$. The first two operators, which are used in this paper, are

$$B_1 = \partial/\partial r + 1/2r - jk \tag{7a}$$

$$B_2 = \partial/\partial r + 1/2r - jk - \left(\partial^2/\partial\varphi^2 + \frac{1}{4}\right)/[2r^2(1/r - jk)]. \tag{7b}$$

These operators appeared in [8], and differ from those in [9] by the inclusion of the $1/r$ term in the denominator of the last term in (7b). The $1/r$ term may be neglected for the TM case, but must be retained for the TE case. Equation (6) has been previously used (with $n = 1, 2$) in conjunction with finite-difference time-marching schemes to close the computational space at some distance from the scatterer while permitting only an acceptably small level of nonphysical wave reflection [8], [9]. Excellent results have been obtained for radiation boundary surfaces only a few space cells from the scatterer for a wide variety of problems.

Now, however, B_n will be applied to U_s *directly on the surface* of the scatterer, instead of at some distance off the scatterer. This permits formal expressions for the normal derivative of the scattered field $\partial U_s/\partial \nu'$ to be obtained via application of (6) on contour C, and setting the right hand side of (6) equal to zero. First, the following replacements are made:

$$\frac{\partial}{\partial r'} \to \frac{\partial}{\partial \nu'}; \quad \frac{1}{r'} \to \zeta(s'); \quad \frac{1}{r'^2}\frac{\partial^2}{\partial\varphi'^2} \to \frac{\partial^2}{\partial s'^2} \tag{8}$$

where $\zeta(s')$ is the curvature of the cylinder's surface at s', and $\partial^2/\partial s'^2$ is the second derivative with respect to the arc length of C. Essentially, these replacements are motivated by approximating C at a point $\bar{x}(s')$ by its osculating circle [15] and locally defining the operator B_n. Then, $B_1 U_s = 0$ implies

$$\frac{\partial U_s}{\partial \nu'} = [jk - \zeta(s')/2]\, U_s \tag{9a}$$

while $B_2 U_s = 0$ gives

$$\frac{\partial U_s}{\partial \nu'} = \left\{ jk - \frac{\zeta(s')}{2} + \frac{j\zeta^2(s')}{8[k + j\zeta(s')]} \right\} U_s + \frac{j}{2[k + j\zeta(s')]} \frac{\partial^2 U_s}{\partial s'^2}. \tag{9b}$$

Since the cylinder is perfectly conducting, U_s is replaced by $-U_{\rm inc}$ on the right hand side of (9). This gives, for B_1 and B_2, respectively,

$$\frac{\partial U_s}{\partial \nu'} = \left[\frac{\zeta(s')}{2} - jk\right] U_{\rm inc}, \quad \text{for } B_1 \tag{10a}$$

$$\frac{\partial U_s}{\partial \nu'} = \left\{ \frac{\zeta(s')}{2} - jk - \frac{j\zeta^2(s')}{8[k + j\zeta(s')]} \right\} U_{\rm inc} - \frac{j}{2[k + j\zeta(s')]} \frac{\partial^2 U_{\rm inc}}{\partial s'^2}, \quad \text{for } B_2. \tag{10b}$$

Inserting either of these results into (3a) gives an analytical formula for the scattered field. The corresponding surface electric current expressions are obtained by combining (3b) with either (10a) or (10b).

We observe that the term $-jkU_{\rm inc}$, which appears in both (10a) and (10b), is the leading-order Kirchoff term. In the OSRC formulation, however, this term as well as the others is valid in both the lit and shadow regions of a convex scatterer.

III. Application to the Circular Cylinder: TM Polarization

This section will discuss the application of the on-surface radiation condition formulation to the first of three canonical, two-dimensional, convex conducting geometries, the circular cylinder for TM polarization of the incident wave. For this problem, C is the circle $r = 1$, with $\partial/\partial\nu' = \partial/\partial r'$, $\zeta = 1$, and the s' derivatives in (10b) are just φ' derivatives. Without loss of generality, α is taken as zero in (1) so that (10a) and (10b) become

$$\frac{\partial U_s}{\partial r'} = \left(\frac{1}{2} - jk\right) e^{jk\cos\varphi'}, \quad \text{for } B_1 \tag{11a}$$

$$\frac{\partial U_s}{\partial r'} = \left(\frac{1}{2} - jk - \frac{j}{8k} - \frac{1}{2}\cos\varphi' + \frac{jk}{2}\sin^2\varphi'\right) e^{jk\cos\varphi'}, \quad \text{for } B_2. \tag{11b}$$

In (11b), the term $(k + j\zeta)$ in (10b) has been replaced by k. Computed results for the surface current obtained using these expressions and (3b) are shown in Fig. 1(a) for $k = 5$, and in Fig. 1(b) for $k = 10$, along with the results obtained by using a cylindrical mode summation. As is evident, (11b) agrees with the modal sum more closely than (11a). In general, the use of the higher order B_2 operator implied by (11b) results in agreement of the surface current to within 1 dB of the exact solution for the $k = 10$ case.

Inserting (11a) and (11b) into (5) gives, after some manipulation, the following respective formulas for bistatic radar cross section:

$$\frac{\rm RCS}{\lambda} = \frac{k^2\pi}{2} \cdot \left| \left(j - \frac{1}{2k}\right) J_0(\xi) + \sin(\varphi/2) J_1(\xi) \right|^2, \quad \text{for } B_1 \tag{12a}$$

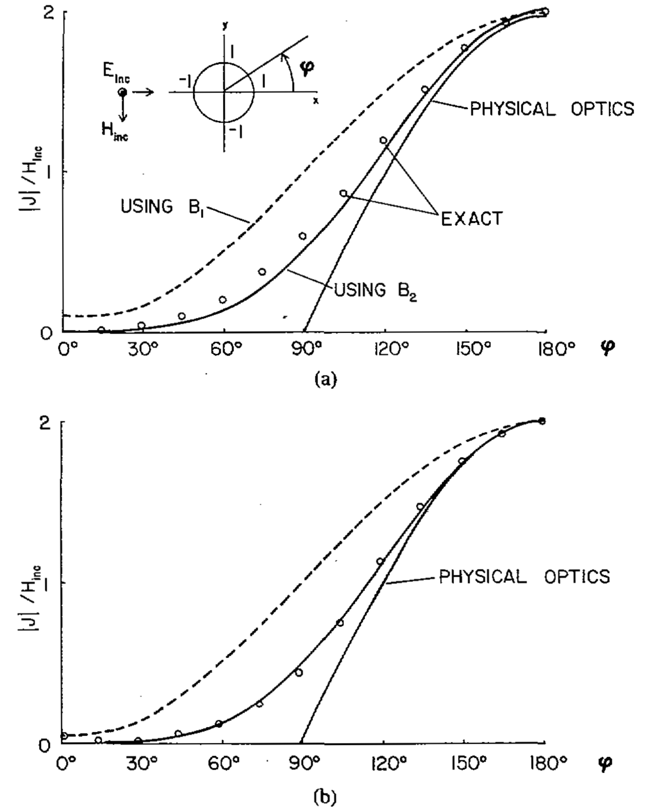

Fig. 1. Surface electric current on conducting circular cylinder, TM case, computed using OSRC method, showing convergence to exact solution for higher order radiation boundary operator. (a) $k = 5$. (b) $k = 10$.

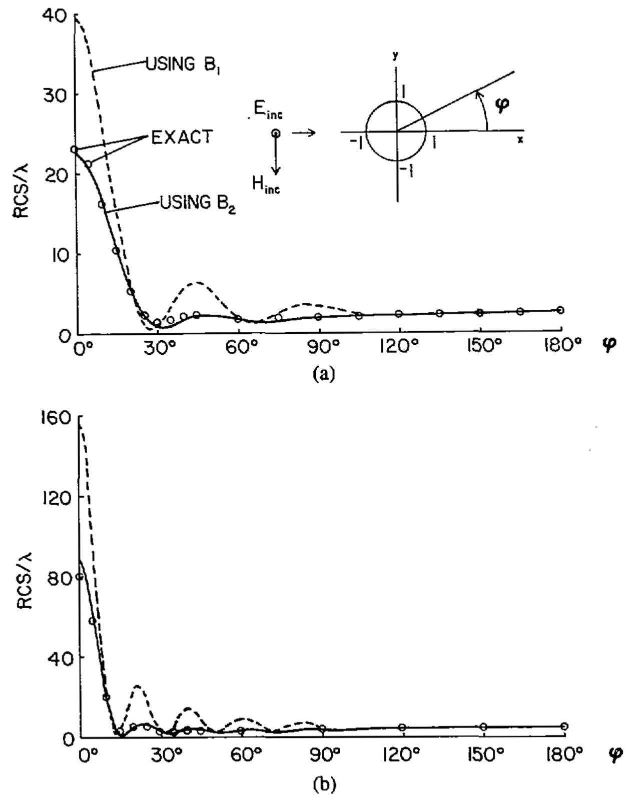

Fig. 2. Bistatic radar cross section of conducting circular cylinder, TM case, computed using OSRC method, showing convergence to exact solution for higher order radiation boundary operator. (a) $k = 5$. (b) $k = 10$.

$$\frac{\text{RCS}}{\lambda}=\frac{k^2\pi}{2}\cdot\left|\left[j-\frac{1}{2k}-\frac{j}{2}\cos^2(\varphi/2)\right]J_0(\xi)+g(\varphi)J_1(\xi)\right|^2,\quad \text{for } B_2 \tag{12b}$$

where

$$g(\varphi)\equiv\left(1+\frac{j}{2k}\right)\sin(\varphi/2)+\frac{\cos\varphi}{2\xi} \tag{12c}$$

$$\xi\equiv 2k\sin(\varphi/2). \tag{12d}$$

Note that the evaluation of only two Bessel functions is required for the RCS computation, regardless of the electrical size of the cylinder.

Fig. 2(a) shows the magnitudes of the radar cross section computed using (12a) and (12b) for the $k = 5$ cylinder case, along with the exact solution. Fig. 2(b) plots corresponding data for the $k = 10$ cylinder case. Just as observed in Figs. 1(a) and 1(b) (cylinder surface currents), the radar cross section obtained using the formula corresponding to the higher order radiation condition B_2, is in much better agreement with the exact solution than that corresponding to B_1. Here, the higher order formula, (12b), results in agreement to within 0.5 dB of the exact radar cross section, in general.

IV. Application to the Conducting Strip: TM Polarization

In this example, the scatterer surface contour C is composed of the upper and lower halves of the line segment $y = 0$, $|x| \leq 1$. On the upper half of the strip, $\partial/\partial\nu' = \partial/\partial y'$, $\zeta = 0$, and $\partial^2/\partial s'^2 = \partial^2/\partial x'^2$; while on the lower half of the strip, $\partial/\partial\nu' = -\partial/\partial y'$. No special attention or care is paid to the edges, $x' = \pm 1$, $y' = 0$ although the edges are points of infinite curvature. For brevity, only the higher order normal derivative expression, (10b), will be used in this example. Inserting (1) into (10b) gives

$$\frac{\partial U_s}{\partial\nu'}=-jk\left(1-\frac{1}{2}\cos^2\alpha\right)e^{jkx'\cos\alpha},\quad \text{for } B_2. \tag{13a}$$

Using (13a) and (3b), the z-directed surface electric current is given by

$$J=\frac{1}{\eta_0}\left(\pm\sin\alpha+1-\frac{1}{2}\cos^2\alpha\right)e^{jkx'\cos\alpha},\quad \text{for } B_2(\text{at } y=0\pm). \tag{13b}$$

Note that for a given wave angle of incidence α, the magnitude of J is independent of position x' on the strip, similar to the physical optics case. However, a nonzero value of J is computed in the shadow region $y = 0-$.

Inserting (13a) into (5) with $\varphi = \pi - \alpha$ gives

$$\frac{\text{RCS}}{\lambda}=\frac{1}{2\pi}\cdot\left|\left(1-\frac{1}{2}\cos^2\alpha\right)\frac{\sin(2k\cos\alpha)}{\cos\alpha}\right|^2;\quad \text{for } B_2 \tag{14}$$

as the monostatic radar cross section of the conducting strip.

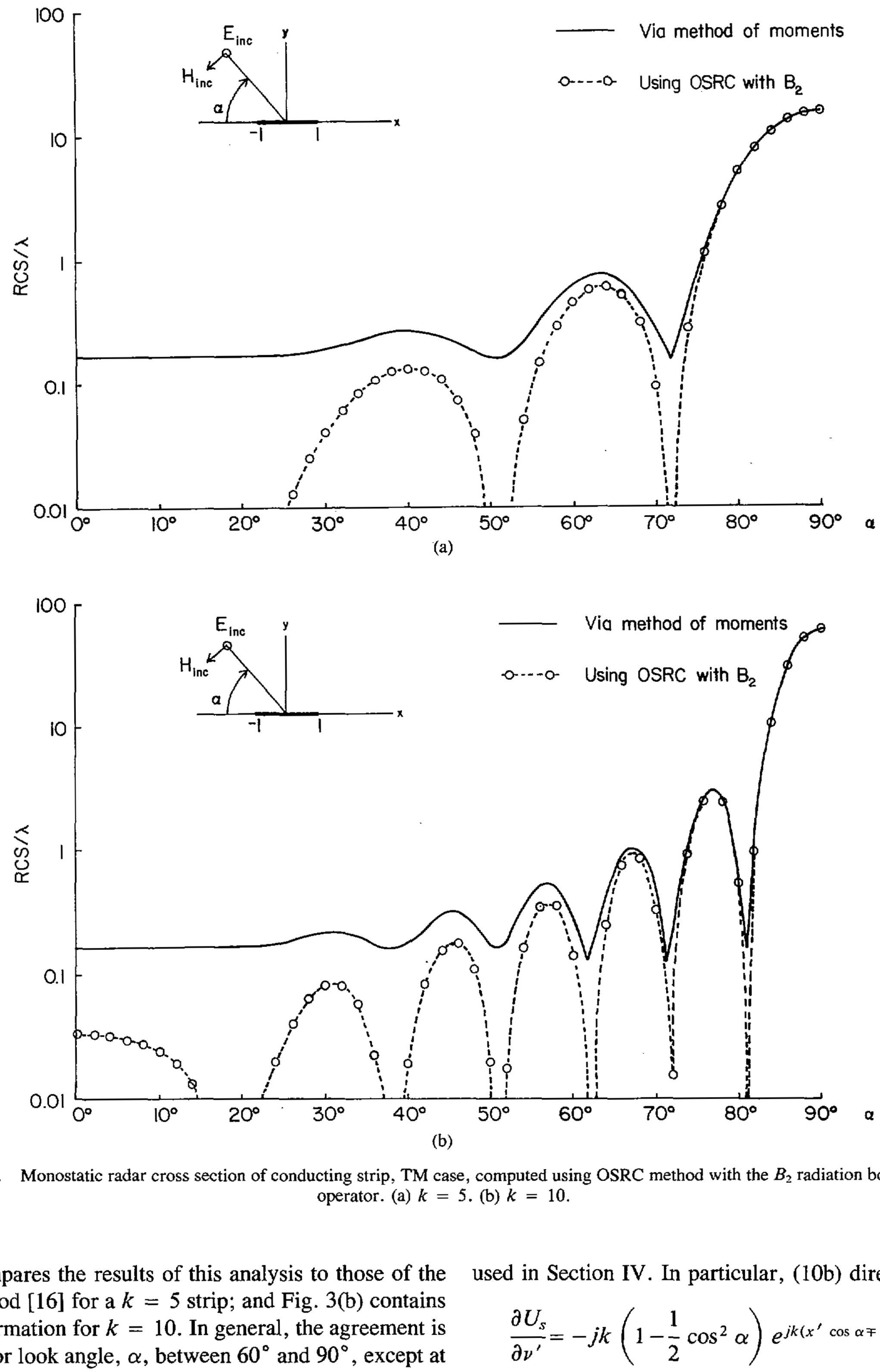

Fig. 3. Monostatic radar cross section of conducting strip, TM case, computed using OSRC method with the B_2 radiation boundary operator. (a) $k = 5$. (b) $k = 10$.

Fig. 3(a) compares the results of this analysis to those of the moment method [16] for a $k = 5$ strip; and Fig. 3(b) contains the same information for $k = 10$. In general, the agreement is within 1 dB for look angle, α, between 60° and 90°, except at nulls. Disagreement at smaller α is probably due to edge currents.

V. Application to the Square Conducting Cylinder: TM Polarization

In this example, the scatterer surface contour C is a square with the four corners $(\pm\sqrt{2}, \pm\sqrt{2})$. The determination of the surface current distribution follows the same line of analysis as used in Section IV. In particular, (10b) directly gives

$$\frac{\partial U_s}{\partial \nu'} = -jk\left(1 - \frac{1}{2}\cos^2\alpha\right) e^{jk(x'\cos\alpha \mp \sin\alpha)}, \quad \text{for } B_2 \tag{15a}$$

for $|x| \leqq 1$, $y = \pm 1$; and

$$\frac{\partial U_s}{\partial \nu'} = -jk\left(1 - \frac{1}{2}\sin^2\alpha\right) e^{jk(\pm\cos\alpha - y'\sin\alpha)}; \quad \text{for } B_2 \tag{15b}$$

for $x = \pm 1$, and $|y| \leqq 1$. The z-directed surface electric current follows from (15a), (15b), and (3b). It is given by

$$J=\frac{1}{\eta_0}\left(\pm \sin \alpha+1-\frac{1}{2} \cos^2 \alpha\right) e^{jk(x' \cos \alpha \mp \sin \alpha)}, \quad \text{for } B_2 \tag{16a}$$

for $|x| \leqq 1$, $y = \pm 1$; and

$$J=\frac{1}{\eta_0}\left(\mp \cos \alpha+1-\frac{1}{2} \sin^2 \alpha\right) e^{jk(\pm \cos \alpha - y' \sin \alpha)}, \quad \text{for } B_2 \tag{16b}$$

for $x = \pm 1$, and $|y| \leqq 1$. Similar to the strip case of Section IV, it is noted that, for a given wave angle of incidence α the magnitude of J is independent of position, x' or y', on each side of the cylinder. It is also noted that nonzero values of J are computed in the shadow regions of the cylinder.

To compute the monostatic radar cross section, (15a) and (15b) are inserted into (5) with $\varphi = \pi - \alpha$:

$$\frac{\text{RCS}}{\lambda}=\frac{1}{2\pi} \cdot |g_1(\alpha)+g_2(\alpha)+g_3(\alpha)|^2 \tag{17a}$$

where

$$g_1(\alpha)=\left(1-\frac{1}{2} \sin^2 \alpha\right) \frac{\sin (2k \sin \alpha)}{\sin \alpha} \cos (2k \cos \alpha) \tag{17b}$$

$$g_2(\alpha)=\left(1-\frac{1}{2} \cos^2 \alpha\right) \frac{\sin (2k \cos \alpha)}{\cos \alpha} \cos (2k \sin \alpha) \tag{17c}$$

$$g_3(\alpha)=\frac{-j \sin (2k \sin \alpha) \sin (2k \cos \alpha)}{\sin \alpha \cos \alpha}. \tag{17d}$$

The formula for the monostatic radar cross section versus α is now given by (17a). Results using this formula are shown in Figs. 4(a) and 4(b) in comparison with the method of moments [16] for the $k = 5$ and $k = 10$ cylinder cases. Agreement is within about 0.5 dB at all points (except for $\alpha = 12°$ and $\alpha = 14°$ for the $k = 10$ case).

VI. Formulation of the OSRC Approach (TE Polarization)

For the case of TE polarization, (2b) is still valid if U_s is identified as the scattered z-directed magnetic field. Now, however, the surface current is given in terms of the incident field, i.e., $\partial U_s/\partial \nu'$ is known in (2b). If B_1 is used, (9a) would then give U_s on C, and (2b) would be an analytic formula for $U_s(\bar{x})$. If the higher order B_2 expression of (9b) is used, then $U_s[\bar{x}'(s')]$ satisfies a linear second-order differential equation. By requiring that the solution be L-periodic (L is the dimensionless length of C; L-periodic means that the solution must be observed to repeat itself upon successive complete walks around C), and noting that the coefficient of U_s is not purely complex, a unique solution of (9b) can be found. When this is inserted into (2b), once again an analytic formula for $U_s(\bar{x})$ can be obtained.

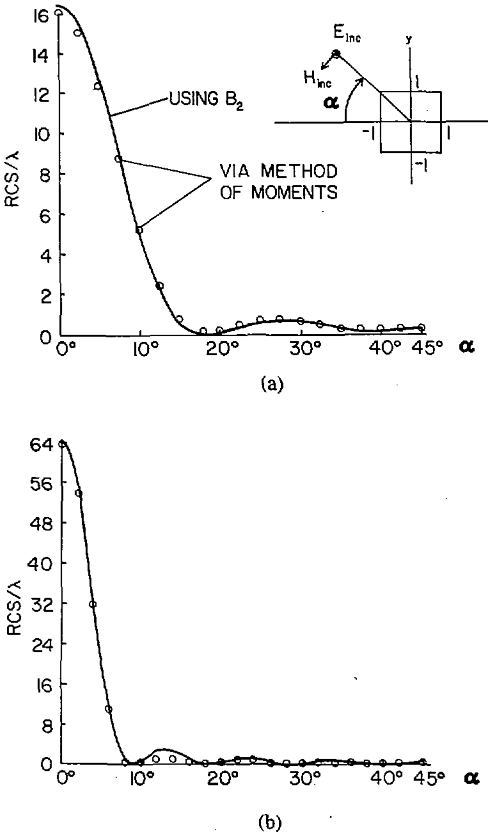

Fig. 4. Monstatic radar cross section of conducting square cylinder, TM case, computed using OSRC method with the B_2 radiation boundary operator. (a) $k = 5$. (b) $k = 10$.

Let us now apply the above to the case of the circular conducting cylinder. For convenience, the definitions of Section III will again be used. For TE polarization, we have

$$J_\varphi = -(U_s + U_{\text{inc}}) \tag{18a}$$

and

$$\frac{\partial U_s}{\partial \nu'} = -\frac{\partial U_{\text{inc}}}{\partial \nu'}. \tag{18b}$$

On substituting (18a) and (18b) into (9a), the total surface electric current on the circular cylinder is obtained as

$$J_\varphi = -U_{\text{inc}} \cdot (1-\cos \varphi), \quad \text{for } B_1. \tag{19}$$

Note that the use of B_1 provides an explicit expression for the current.

The case for B_2 is more involved. Substituting (18a) and (18b) into (9b) yields the following second-order differential

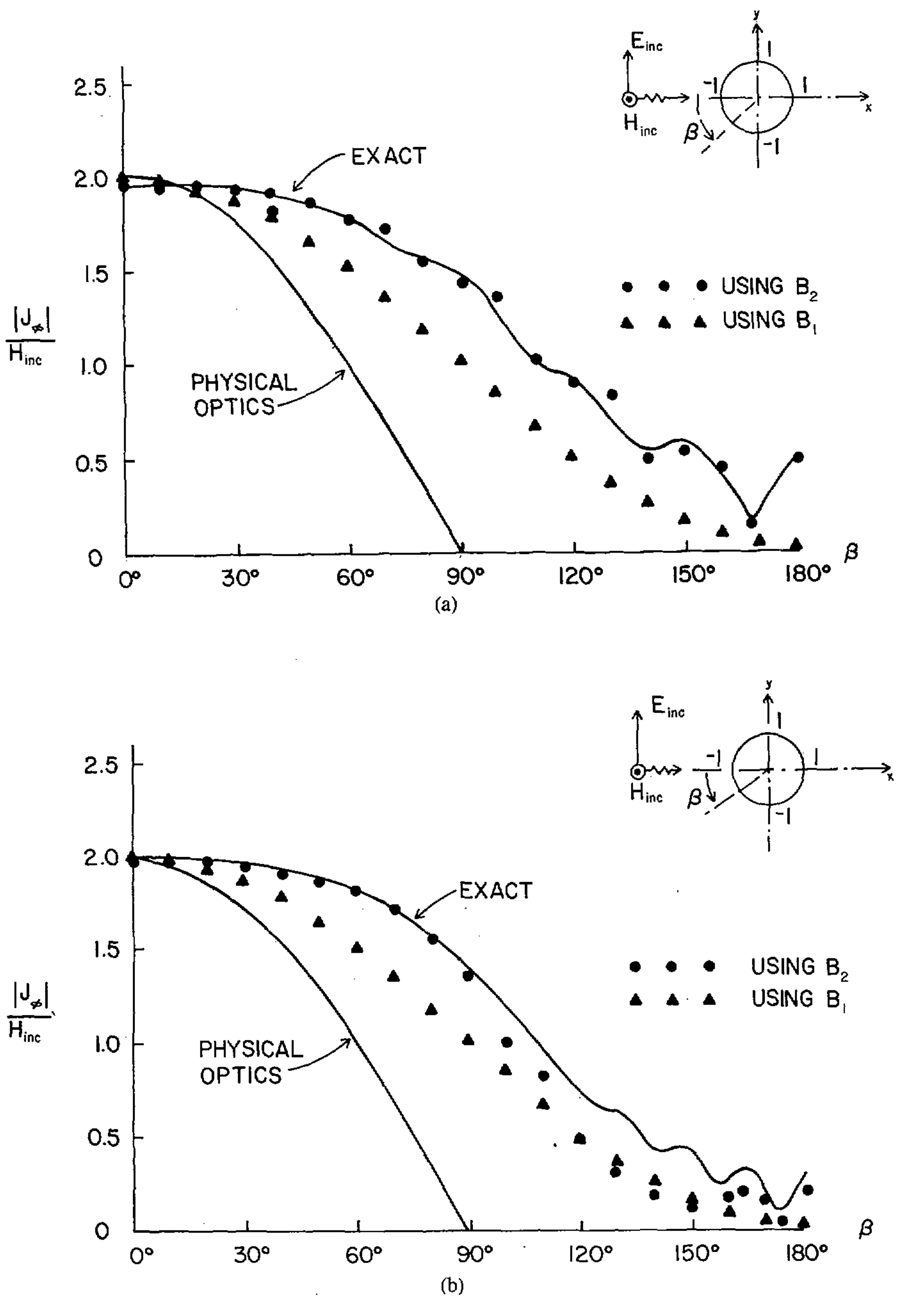

Fig. 5. Surface electric current on conducting circular cylinder, TE case, computed using OSRC method, showing convergence to exact solution for higher order radiation boundary operator. (a) $k = 5$. (b) $k = 10$.

equation for the current:

$$C_2 \frac{d^2 J_\varphi}{d\varphi^2} - J_\varphi = U_{\text{inc}} \cdot (1 - C_1 \cos \varphi) - C_2 \frac{\partial^2 U_{\text{inc}}}{\partial \varphi^2}, \quad \text{for } B_2 \tag{20a}$$

where

$$C_1 = \frac{8k^2 + j8k}{-3 + 8k^2 + j12k}; \quad C_2 = \frac{-4}{-3 + 8k^2 + j12k} \tag{20b}$$

and J_φ is 2π-periodic. We note that this system is linear with constant coefficients, and can be solved using standard analytical or numerical methods. We also note from (20) that, in the high-frequency limit (large k), C_1 approaches 1 and C_2 approaches $-1/2k^2$. However, (20) does not reduce to (19) because the φ derivatives introduce k^2 factors multiplying the C_2 terms.

Fig. 5 graphs the B_1 OSRC solution (from (19)), the B_2 OSRC solution (from the system of (20)), and the method of moments solution for the current distribution on a $k = 5$ and $k = 10$ cylinder. Note that the use of the B_2 operator extends the range of essential agreement between OSRC and the method of moments result over most of the circumference of the cylinder. In particular, we observe the evolution of an oscillatory behavior (identified as the result of the creeping wave) in the shadow region.

When the scattering cylinder is convex but not circular, the system of (20) no longer has constant coefficients. Again, there are standard solution techniques. In particular, a simple and very promising approach is the following iterative scheme, illustrated for (20) as

$$J_{\varphi}^{(n+1)}=C_2 \frac{d^2 J_{\varphi}^{(n)}}{d\varphi^2}-U_{\text{inc}} \cdot (1-C_1 \cos \varphi)+C_2 \frac{\partial^2 U_{\text{inc}}}{\partial \varphi^2} \quad (21)$$

where $J^{(n)}$ denotes the nth iteration for the current. A convenient selection for $J_{\varphi}^{(0)}$ is the B_1 result given by (19). This scheme would be conveniently implemented for arbitrary convex bodies on conventional computers.

VII. Relation to Previous High-Frequency Approaches

The OSRC approach provides an approximate asymptotic high-frequency result which is convenient for engineering applications. This new approach is valid both for fields directly at the surface and exterior to the surface of a smooth, perfectly conducting, convex cylinder when it is illuminated by a plane wave. As was seen for the $k = 5$ and $k = 10$ circular cylinders, the computed surface current result is uniform in the sense that it remains essentially valid within the transition region between lit and shadow regions, and even in deep shadow regions. As observed earlier, the OSRC results contain the leading-order Kirchoff term, as well as others, which are valid in both lit and shadow regions.

Previous work in this area [17], [18] also developed uniform-theory solutions for convex, conducting, two-dimensional cylinders. However, the previous work required a complicated analysis. In fact, a separate analysis was needed close to the cylinder surface. The new approach discussed in this paper has the advantages of simplicity and a consistent ease of application for arbitrary convex cylinders, for both on-surface and off-surface fields. Further, the new approach appears to permit good treatment of convex scatterers that do not have smooth surface contours, i.e., have edges or corners, as exemplified by the strip and square-cylinder results reported in this paper. Shadow-region currents with OSRC are nonzero for such structures. However, OSRC does not currently provide edge-current singularity behavior.

VIII. Summary and Conclusion

A new formulation of electromagnetic wave scattering by two-dimensional conducting bodies of convex shape has been presented. This formulation is based upon a series expansion of the radiation condition which is applied directly on the scatterer surface. Substantial simplification of the overall scattering formulation is achieved since the original integral equation for the scattered field is reduced to just a line integral whose integrand is either known (for the TM case) or can be easily constructed (for the TE case). Results presented for TM illumination of the circular cylinder, square cylinder, and infinitely thin strip scatterers are simple analytical expressions for the surface electric current distribution and radar cross section. Results presented for TE illumination of the circular cylinder are obtained via solution of a simple second-order differential equation. Comparison of these OSRC results with benchmark computations for scatterer sizes of $ka = 5$ and $ka = 10$ indicates good agreement for the B_2 radiation operator.

The ability to easily construct a sequence of higher order OSRC operators may ultimately lead to new approaches in modeling reentrant scatterers (as well as convex) and three-dimensional scatterers. This may present a useful alternative to present integral equation and uniform high-frequency approaches for such structures. A forthcoming paper will consider the application of OSRC to convex dielectric scatterers [1].

Acknowledgment

The authors wish to thank the referees for their constructive remarks. They also wish to thank Mr. Thomas Moore for his careful checking of the analysis and numerical implementation.

References

[1] K. R. Umashankar, A. Taflove, and G. A. Kriegsmann, "Extension of on-surface radiation condition theory to scattering by two-dimensional homogeneous dielectric objects," *IEEE Trans. Antennas Propagat.*, submitted for publication.

[2] A. C. Vastano and R. O. Reid, "Tsunami response for islands: verification of a numerical procedure," *J. Marine Research*, vol. 25, pp. 129–139, 1967.

[3] D. E. Merewether, "Transient currents induced on a metallic body of revolution by an electromagnetic pulse," *IEEE Trans. Electromagn. Compat.*, vol. EMC-13, pp. 41–44, May 1971.

[4] K. S. Kunz and K.-M. Lee, "A three-dimensional finite-difference solution of the external response of an aircraft to a complex transient EM environment: Part I—The method and its implementation," *IEEE Trans. Electromagn. Compat.*, vol. EMC-20, pp. 328–333, May 1978.

[5] G. A. Kriegsmann and C. S. Morawetz, "Numerical solutions of exterior problems with the reduced wave equation," *J. Comp. Phys.*, vol. 28, pp. 181–197, 1978.

[6] E. L. Lindman, "Free-space boundary conditions for the time dependent wave equation," *J. Comp. Phys.*, vol. 18, pp. 66–78, 1975.

[7] B. Engquist and A. Majda, "Absorbing boundary conditions for the numerical simulation of waves," *Math. Comp.*, vol. 31, pp. 629–651, July 1977.

[8] G. A. Kriegsmann and C. Morawetz, "Solving the Helmholtz equation for exterior problems with variable index of refraction: I," *SIAM J. Sci. Stat. Comput.*, vol. 1, pp. 371–385, Sept. 1980.

[9] A. Bayliss and E. Turkel, "Radiation boundary conditions for wave-like equations," *Commun. Pure Appl. Math.*, vol. 33, pp. 707–725, 1980.

[10] G. Mur, "Absorbing boundary conditions for the finite-difference approximation of the time-domain electromagnetic field equations," *IEEE Trans. Electromagn. Compat.*, vol. EMC-23, pp. 377–382, Nov. 1981.

[11] L. N. Trefethen and L. Halpern, "Well-posedness of one-way wave equations and absorbing boundary conditions," Inst. Comput. Appl. Sci. and Eng. (ICASE), NASA Langley Res. Center, Hampton, VA, Rep. 85-30, June 1985.

[12] K. R. Umashankar and A. Taflove, "A novel method to analyze electromagnetic scattering of complex objects," *IEEE Trans. Electromagn. Compat.*, vol. EMC-24, pp. 397–405, Nov. 1982.

[13] A. Taflove and K. R. Umashankar, "Radar cross section of general three-dimensional scatterers," *IEEE Trans. Electromagn. Compat.*, vol. EMC-25, pp. 433–440, Nov. 1983.

[14] A. Taflove, K. R. Umashankar, and T. G. Jurgens, "Validation of FD-TD modeling of the radar cross section of three-dimensional structures spanning up to nine wavelengths," *IEEE Trans. Antennas Propagat.*, vol. AP-33, pp. 662–666, June 1985.

[15] J. J. Stoker, *Differential Geometry*. New York: Wiley, 1969.

[16] R. F. Harrington, *Field Computation by Moment Methods*. New York: Macmillan, 1968.

[17] R. Kouyoumjian, "Asymptotic high-frequency methods," *Proc. IEEE*, vol. 53, pp. 864–876, Aug. 1965.

[18] P. H. Pathak, "An asymptotic analysis of the scattering of plane waves by a smooth convex cylinder," *Radio Sci.*, vol. 14, pp. 419–435, May-June 1979.

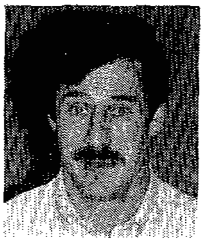

Gregory A. Kriegsmann received the M.S. degree in electrical engineering and the Ph.D. degree in applied mathematics from the University of California, Los Angeles, in 1970 and 1974, respectively.

He was a Courant Instructor in Applied Mathematics at New York University from 1974 to 1976. He is currently Professor of Applied Mathematics in the Department of Engineering Sciences and Applied Mathematics at Northwestern University, Evanston, IL. His research interests include the development of asymptotic and numerical methods for solving wave propagation problems.

Dr. Kriegsmann is a member of Tau Beta Pi, the Society of Industrial and Applied Mathematicians, and the Acoustical Society of America.

Allen Taflove (M'75–SM'84), for a photograph and biography please see page 766 of the June 1986 issue of this TRANSACTIONS.

Korada R. Umashankar (S'69–M'75–SM'81), for a photograph and biography please see pages 765 and 766 of the June 1986 of this TRANSACTIONS.